Importance of MUC17 in the Bile-Induced Pancreatic Cancer Progression

Eleonóra Gál
University of Szeged
István Menyhárt
University of Szeged
Zoltán Veréb
University of Szeged
László Tiszlavicz
University of Szeged
Tamás Takács
University of Szeged
László Czakó
University of Szeged
Péter Hegyi
Semmelweis University
Viktoria Venglovecz (venglovecz.viktoria@med.u-szeged.hu)
University of Szeged

Research Article

Keywords: pancreatic cancer, obstructive jaundice, MUC17, MUC4, bile acids

Posted Date: February 18th, 2022

DOI: https://doi.org/10.21203/rs.3.rs-1357586/v1

Abstract

We have previously shown that bile acids (BAs) accelerate carcinogenic processes in pancreatic cancer (PC) in which mucin 4 (MUC4) expression has a central role. However, the roles of other mucin isoforms in PC are less clear, especially in bile-induced cancer progression. The study aim was to investigate expression of MUC17 in a BAs- or human serum-treated pancreatic ductal adenocarcinoma (PDAC) cell line and use different assays with RNA silencing to study the role of MUC17 in cancer progression. Protein expression of MUC17 was evaluated in 52 human pancreatic samples by immunohistochemistry, and Kaplan–Meier survival analysis was used to compare survival curves. Expression of MUC17 increased in PDAC patients, especially in obstructive jaundice (OJ). A significant association was found between elevated MUC17 expression and poorer overall survival in the PDAC + OJ group. Treatment of PDAC cells with BAs or with human serum obtained from PDAC + OJ patients enhanced the expression of MUC17, whereas knockdown of MUC17 alone or in combination with MUC4 decreased BAs-induced carcinogenic processes. Our results demonstrated that MUC17 has a central role in bile-induced PC progression, and in addition to MUC4, this isoform also can be used as a novel prognostic biomarker.

Introduction

Pancreatic cancer (PC) is one of the most aggressive cancers throughout the world [1]. A common consequence of PC is bile-duct obstruction, which decreases quality of life and contributes to poor outcome [2]. Several mechanisms have a role in the negative effects of bile, one of which is the altered expression of mucins. Mucins are high molecular-weight glycosylated proteins that have a crucial role in the physical protection of the underlying epithelial layer. Secreted and transmembrane mucins can be distinguished by their structural and functional properties. Secreted mucins are major components of the mucin layer, whereas transmembrane mucins are located on the apical surface of epithelial cells and play an important role in maintaining mucosal barrier function [3]. Twenty-one mucin genes have been identified so far, of which, the altered expressions of Mucin (MUC)1, -4, and − 5AC have been shown to predict PC progression and outcome [4,5]. Although obstructive jaundice (OJ) is present in roughly 70% of PC patients,[2] the effect of bile acids (BAs) has only been studied on the MUC4 isoform [6,7]. We have previously shown that BAs increase the tumorigenic potential of pancreatic ductal adenocarcinoma (PDAC) cells through overexpression of MUC4 [6]. Increased expression of this isoform also has been detected in PDAC patients associated with OJ, and in this case, the 4-year overall survival rate was significantly worse [6]. In contrast, the effect of BAs on the other mucin isoforms has not been investigated; however, understanding the molecular mechanisms that are involved in bile-induced cancer progression can help in the development of more effective therapies, and on the other hand, can contribute to identification of diagnostic biomarkers for more accurate and broader assessment of PC progression.

The study aim was to investigate expression of MUC17 in a BAs- or human serum-treated pancreatic ductal adenocarcinoma (PDAC) cell line and use different assays with RNA silencing to study the role of

MUC17 in cancer progression. We showed for the first time that BAs upregulated *MUC17* expression in PC and that high expression of this isoform significantly impaired survival in OJ-associated PC patients.

Results

High MUC17 expression is related to lower survival

MUC17 staining was not or was only slightly detected in the normal pancreas and neuroendocrine tumors. In contrast, strong expression of MUC17 was observed in PDAC, especially in the apical membrane of intra- and interlobular ducts (Figure 1A and B). The presence of OJ further increased MUC17 expression in the PDAC groups, but there were no significant differences in sex, age, location of primary tumor, histological type, stage, lymphatic invasion, or metastasis between the PDAC and PDAC + OJ groups (Table 1). In the next step, we examined the association between MUC17 expression and median survival of the patients. Based on the intensities of MUC17 staining, we distinguished weak, moderate, and strong groups. In the PDAC + OJ group, strong expression of MUC17 was associated with the worst survival (Figure 1C). In the PDAC group, only weak and moderate MUC17 staining was detected, and there were no significant differences between the groups. We have previously shown a similar correlation between MUC4 positivity and poor patient prognosis, so we also investigated how dual positivity affects median survival. In the PDAC + OJ group, MUC4 and -17 positivity greatly reduced median survival (9.5 ± 2.44) relative to survival in patients who showed only MUC4 (15.05 ± 2.03) or MUC17 (13.45 ± 1.87) positivity (Figure 1C and D). Interestingly, better survival was observed for double positivity in the PDAC group than in the other groups, although no significant difference was detected. Comparison of the PDAC and PDAC + OJ groups showed that the presence of OJ worsened disease outcome in line with our previous observation [6].

Bile acids upregulate the expression of MUC17

Since MUC17 staining was significantly stronger in the PDAC + OJ group, we hypothesized that BAs affect MUC17 expression. To confirm this hypothesis, the Capan-1 PDAC cell line was treated with serum obtained from PDAC and PDAC + OJ patients for 24, 48, and 72 h, and the mRNA expression of MUC17 was investigated by reverse transcriptase-polymerase chain reaction (RT-PCR). As a control, serum from healthy volunteers was used. Serum from PDAC + OJ patients induced a several-fold increase in MUC17 expression after 72 h of incubation (Figure 2A). In contrast, only a small increase was detected in PDAC serum. One of the major differences between the two serums was that the total BA concentration was significantly higher in patients with OJ,[6] which suggests that bile has a key role in MUC17 overexpression in PDAC + OJ patients. To validate this hypothesis and to identify which BAs are involved, Capan-1 cells were pre-treated with the most common BAs (100 and 500 μM) for 24, 48, and 72 h and the mRNA expression of MUC17 was investigated (Figure 2B). Among the BAs, TCDCA induced a robust increase (approx. 5-fold compared with the control) in the expression of MUC17 at a high concentration (500 μM) for all incubation times (Figure 2B). TCDCA also increased MUC17 expression at

the protein level as shown in Figures 2C and D. In addition, gene cluster analysis has shown that the expression of MUC17 is correlated with the expression of MUC4 in the TCDCA-treated group (Figure 2E).

MUC17 promotes PC progression

Next, we have investigated the effect of MUC17 knockdown on the proliferation of Capan-1 cells. MUC17 was silenced by MUC17-specific siRNA, and the efficiency of MUC17 knockdown was confirmed by RT-PCR and ICC (Figure 3A). We found that silencing of MUC17 significantly increased cell death and decreased the rate of proliferation, adhesion, migration, and colony formation in a time-dependent manner (Figure 3B-H). These data indicate that MUC17 has an essential role in the proliferation and metastatic potential of Capan-1 cells. TCDCA treatment resulted in an increase in the aforementioned parameters in the control cell line, whereas no such increase was observed in MUC17 knockdown cells, suggesting that MUC17 protein has an essential role in the action of TCDCA. Similar results were previously found with the MUC4 isoform, so we next investigated the effect of double knockdown. Silencing of both MUC17 and MUC4 reduced the above parameters more strongly than MUC4 or MUC17 knockdown alone. Interestingly, in the case of colony formation, the number of large and extra-large colonies in particular decreased with silencing of MUC4 and/or MUC17, suggesting that these isoforms promote development of larger tumors (Figure 3H). MUC4/17 knockdown prevented the effects of TCDCA on proliferation, adhesion, and migration, whereas in the case of colony formation, a slight increase in the number of large and extra-large colonies was observed.

Discussion

Several studies have reported that mucins have a key role in the progression of different cancer types, so some of them are also thought to be potential biomarkers [8]. Among the mucin isoforms, the presence of MUC4 is strongly associated with PDAC, its expression increases as the disease progresses, and it contributes functionally to the aggressiveness of the disease [9,10]. In our previous study, we showed that MUC4 expression was increased by BAs, which explains the worse outcome of PDAC patients with OJ [6]. Since biliary obstruction is present in approximately 70–90% of PDAC patients and elevated serum bile levels increase mortality and morbidity, it is of great importance to completely understand the molecular mechanisms of bile-induced PC carcinogenesis, which may contribute to the development of new therapies or to the assessment of the course of the disease.

In this study, we showed for the first time that in addition to MUC4, the expression of another mucin isoform, namely MUC17, was also increased by bile. MUC17 is one of the major components of the glycocalyx, and aberrant expression of this isoform has been observed in several types of tumors, including stomach, colon, and pancreas [11–14]. Regarding the pancreas, overexpression of MUC17 has been described in PDAC, and this isoform also has been identified as an independent prognostic factor for poor overall survival [11,12]; however, the underlying mechanism is not completely understood. Kitamo et al. showed that MUC17 expression was largely determined by DNA methylation status and that histone modifications and overexpression of MUC17 were regulated by hypoxia [15,16]. In our study, we found an

association between MUC17 staining and the presence of OJ. MUC17 expression was significantly higher in PDAC + OJ patients than in PDAC patients, indicating that bile regulates MUC17 expression. In addition, the intensity of MUC17 staining was directly proportional to the poorer survival of PDAC patients, as previously shown for MUC1, -4, and − 5AC [4,5]. Importantly, we found that the presence of both MUC4 and − 17 significantly reduced patient survival relative to that for MUC4 or -17 positivity alone, suggesting that the effects of MUC4 and − 17 are additive.

Downregulation of MUC17 resulted in decreased growth and metastasis of PDAC cells, which confirms the central role of MUC17 in PC. Double knockdown of MUC4 and − 17 further reduced these parameters, which is consistent with a poorer outcome in MUC4/17-positive patients. One of our important findings was that silencing of MUC17 was able to counteract the effect of TCDCA on PC cells, and this protective effect was further enhanced in the case of MUC4/17 double knockdown. These data indicate that, similar to MUC4 expression, MUC17 expression is increased in PC and indicates poor prognosis. Interestingly, opposite results have been shown in gastric and colon cancers in which MUC17 has a protective role. In the stomach, high expression of MUC17 is associated with improved prognosis, whereas inflammation or neoplastic transformation of the colon results in decreased MUC17 expression [13,14]. The protective role of MUC17 in the stomach is related to inhibition of the inflammatory response, whereas in the colon, MUC17 is thought to exert its beneficial effect through cell restitution [14,17]. It is not fully understood why MUC17 has a protective role in some organs and contributes to carcinogenesis in others. It is possible that the different glycosylation statuses lead to different roles [18] but further studies are needed.

Taken together, our results showed that MUC17 was highly expressed and correlated with poor prognosis in PC patients with OJ and that this mucin isoform was involved in the tumorigenic effect of bile. These results suggest that in addition to MUC4, MUC17 is another prognostic factor associated with unfavorable prognosis, especially in patients with biliary obstruction, indicating that co-inhibition of MUC4 and − 17 may have a beneficial effect on PC outcome.

Materials And Methods

Chemicals and solutions

TaqMan gene expression assays, MTT 3-(4,5-dimethylthianol-2-yl)-2,5-diphenyltetrazolium bromid, siRNAs for *MUC4* (Cat. No.: AM 16708), and *MUC17* (Cat. No. : AM 16709), an oligofectamine transfection kit, and the rabbit MUC17 polyclonal antibody (Cat #PA5-56805) were obtained from Thermo Fisher Scientific (Waltham, MA, USA). Mouse MUC4 monoclonal IgG1 antibody was ordered from Santa Cruz Biotechnology (Cat. No.: sc-33654; Dallas, TX, USA). A Technical Manual Cell Counting Kit-8 was ordered from Dojindo Molecular Technologies (Rockville, USA). All other laboratory chemicals were ordered from Sigma-Aldrich Kft. (Budapest, Hungary).

Ethical aspects

The clinical part of the study was carried out with the approval of the Ethics Committee of the University of Szeged (No. : 4714), followed by the EU Member States' Directive 2004/23/EC on presumed consent practice for tissue collection, the guidelines of the Helsinki Declaration, and the General Data Protection Regulation (EU) 2016/679. Written informed consent was obtained from all patients and healthy volunteers for sample and data collection.

Pathological characterization of the patients

Immunohistochemistry (IHC) was performed on pancreatic samples obtained from 52 patients and classified into the following groups: 1) PDAC (average age: 63.78 ± 2.8; male/female ratio: 12/9), 2) PDAC + OJ (average age: 69.7 ± 1.8; male/female ratio: 11/9), 3) neuroendocrine tumor (NET) (average age: 72.5 ± 2.05; male/female ratio: 6:1), and 4) control group (average age: 62.75 ± 3.3; male/female ratio: 1:3). All of the samples were obtained from surgical resection or biopsy. Table 1 shows the pathological characterization of the patients.

Cell line and treatment

Capan-1, a human PDAC cell line, was obtained from American Type Culture Collection and cultured in RPMI-1640 media supplemented with 15% fetal bovine serum; 1% L-glutamine, and 2% antimycotic/antibiotic. The medium was replaced every second day, and the cells were seeded at 100% confluency. The cells were used between passages 30–35. The cells were seeded into 25-cm^2 tissue culture flasks or 96-well tissue plates 2 days before the BAs or serum treatment. The BAs treatment was performed with six different types of BAs [glycocholic acid (GCA), taurocholic acid (TCA), taurodeoxycholic acid (TDCA), glycodeoxycholic acid (GDCA), glycochenodeoxycholic acid (GCDCA), and taurochenodeoxycholic acid (TCDCA)] at two different concentrations (100 and 500 μM), for 24, 48, and 72 h. The serum treatment was performed with serum obtained from PDAC patients with OJ (average age: 72.6 ± 9.8; male/female ratio: 5/5) or without OJ (average age: 80 ± 2.5; male/female ratio: 2/3) and from healthy volunteers (average age: 40.9 ± 18.77; male/female ratio: 6/8) (Table 2) at 50X dilution, for 24, 48, and 72 h. The degree of dilution was determined based on our previous results [6].

Cell-adhesion assay

Tissue plates (96 wells) were coated with 40 μg/ml type 1 collagen from rat-tail in phosphate-buffered saline (PBS) at 4ºC, then 100 μl of the cell suspension (10^5 cells/ml) was added to each of the coated wells and incubated for 20 min. After washing, the cells were incubated with BAs. After the treatments, 10 μl of MTT substrate was added to each well, and the cells were incubated for an additional 3 h. The MTT-treated cells were then lysed in DMSO, and a FLUOstar OPTIMA Spectrophotometer (BMG Labtech, Ortenberg, Germany) at 560 nm, with background subtraction at 620 nm, was used to measure absorbance.

Cytotoxicity assay

Cytotoxicity assay was performed as previously described [6]. Briefly, 100 μl of cell suspension was seeded into a 96-well plate (2×10^4 cells/well) and allowed to adhere overnight. On the following day, the cells

were incubated with BAs, and then 100 µl of supernatant from each of the wells was carefully transferred to a new 96-well plate containing 100 µl of reaction mixture. We then used a FLUOstar OPTIMA Spectrophotometer (BMG Labtech, Ortenberg, Germany) to measure lactate dehydrogenase (LDH) activity at 490 nm. Calculated the percentage of cytotoxicity using the following formula: Cytotoxicity (%) = (exp. value–low control/high control-low control)*100. Low control determines the LDH activity released from the untreated normal cells (spontaneous LDH release), whereas high control determines the maximum releasable LDH activity in the cells (maximum LDH release). As a positive control, 0.1% Triton-X-100 was used.

Proliferation

For proliferation, 100 µl of cell suspension was seeded into a 96-well plate (5×10^3 cells/well), and then the cells were incubated with BAs. After the treatments, 10 µl of a CCK8 solution was added to each well, and the cells were incubated for an additional 3 h. We used a FLUOstar OPTIMA Spectrophotometer (BMG Labtech, Ortenberg, Germany) to measure absorbance at 450 nm.

Wound healing assay

Cells were seeded onto 24-well cell culture plates at a 2.5×10^5 cell density and allowed to adhere overnight. On the following day, P2 tips were used to gently scratch the confluent monolayer, and the cells were incubated with BAs. Automated time-lapse imaging was performed with an Olympus IX83 inverted microscope and the Olympus ScanR screening platform (Olympus, Japan) upgraded with an OKOLAB incubator system (with a gas, temperature, and humidity controller; Pozzuoli, NA, Italy). Image J software (free) was used to analyze the digital images.

Clonogenic assay

Capan-1 cells (10^3 cells/well) were seeded onto 6-well cell culture plates and allowed to adhere overnight. On the following day, the cells were treated with BAs, and then the normal media was given back. The cells were allowed to grow until day 9 after which the media was removed, and the cells were washed with PBS, fixed with methanol–ethanol solutions (3:1 dilution) and then stained with Giemsa. An Olympus IX83 microscope-based screening platform was used for image acquisition, and the Olympus Cellsense Dimension software was used for automated object detection, classification, and measurement to enumerate colonies organized by the treated and untreated cells.

siRNA silencing

MUC4- and MUC17-targeted siRNA oligonucleotides were used to perform MUC4 and MUC17 silencing. The Oligofectamine™ Transfection Reagent was used to perform transfection following the manufacturer's instructions. Then, 2×10^5 cells per well were seeded onto 6-well plates 1 day before the transfection. MUC4 and/or MUC17-targeted siRNAs were transfected into the cells at 40–50% confluency and incubated for 72 h.

Rt-pcr

A NucleoSpin RNA Kit (Macherey-Nagel, Düren, Germany) was used to isolate the total RNA from the cells. A High-Capacity cDNA Reverse Transcription Kit (Applied Biosystems, Foster City, USA) was used for reverse transcription of 2 µg of RNA. TaqMan RT-PCR assays were used to perform teal-time PCR reactions of samples as previously described [6].

Immunostainings

Immunocytochemistry (ICC) was performed on cytospin preparations as previously described [6]. For the staining procedure, the slides were incubated with MUC17 (1:100 dilutions) or MUC4 (1:100) primary antibodies for 30 min. After incubation, the slides were washed and incubated with secondary antibody (EnVision™ Flex/HPR anti-mouse/rabbit) for 30 min. For visualization, an Ultra View Universal diaminobenzidine (DAB) Detection Kit (EnVision™ Flex DAB) was used, and for nuclear staining, EnVision™ Flex Hematoxylin was used. The Olympus IX83-based system was used to scan all specimens. ImageJ was used to further analyze the images, and the intensities of the pixels of the DAB staining were quantified. In the human pancreatic samples, formalin-fixed and paraffin-embedded tissue specimens were used to analyze for MUC4 and − 17 expressions as previously described [6].

Statistical analysis

Quantitative variables were described as means ± SE. Significant differences between groups were assessed by performing ANOVA, and $p \leq 0.05$ was accepted as indicating statistical significance. The Kaplan–Meier method was used to prepare survival curves, and differences in survival were studied by performing the Log-rank test.

Declarations

ACKNOWLEDGEMENT

This study was supported by the National Research, Development, and Innovation Office (FK123982 and SNN134497 to VV). The work of Zoltán Veréb was supported by the EU-funded Hungarian grant EFOP-3.6.1-16-2016-00008, and the Regenerative Medicine and Cellular Pharmacology Research Laboratory was established through the GINOP-2.3.3-15- 2016-00012 project (co-financed by the European Union and the European Regional Development Fund).

AUTHOR CONTRIBUTIONS

EG performed all of the experiments and analyzed the data. ZV and IM were involved in the wound healing, adhesion, and clonogenic assays; siRNA silencing; and quantification of fluorescence intensity. LT evaluated the human pancreas slices and assisted in the immunostainings. Human serum samples

were provided by TT and LC. VV supervised the project and drafted the manuscript. All authors approved the final version of the manuscript.

DATA AVAILABILITY STATEMENT

All data used to support the findings of this study are included within the article.

CONFLICT OF INTEREST

The authors declare that the research was conducted in the absence of any commercial or financial relationships that could be construed as a potential conflict of interest.

References

1. Rawla, P., Sunkara, T. & Gaduputi, V. Epidemiology of Pancreatic Cancer: Global Trends, Etiology and Risk Factors. World J Oncol **10**, 10–27, doi:10.14740/wjon1166 (2019).
2. Boulay, B. R. & Birg, A. Malignant biliary obstruction: From palliation to treatment. World J Gastrointest Oncol **8**, 498–508, doi:10.4251/wjgo.v8.i6.498 (2016).
3. Corfield, A. P. Mucins: a biologically relevant glycan barrier in mucosal protection. Biochim Biophys Acta **1850**, 236–252, doi:10.1016/j.bbagen.2014.05.003 (2015).
4. Suh, H., Pillai, K. & Morris, D. L. Mucins in pancreatic cancer: biological role, implications in carcinogenesis and applications in diagnosis and therapy. Am J Cancer Res **7**, 1372–1383 (2017).
5. Wang, S., You, L., Dai, M. & Zhao, Y. Mucins in pancreatic cancer: A well-established but promising family for diagnosis, prognosis and therapy. J Cell Mol Med **24**, 10279–10289, doi:10.1111/jcmm.15684 (2020).
6. Gal, E. *et al.* Bile accelerates carcinogenic processes in pancreatic ductal adenocarcinoma cells through the overexpression of MUC4. Sci Rep **10**, 22088, doi:10.1038/s41598-020-79181-6 (2020).
7. Joshi, S. *et al.* Bile acids-mediated overexpression of MUC4 via FAK-dependent c-Jun activation in pancreatic cancer. Mol Oncol **10**, 1063–1077, doi:10.1016/j.molonc.2016.04.007 (2016).
8. Kufe, D. W. Mucins in cancer: function, prognosis and therapy. Nat Rev Cancer **9**, 874–885, doi:10.1038/nrc2761 (2009).
9. Chaturvedi, P. *et al.* MUC4 mucin potentiates pancreatic tumor cell proliferation, survival, and invasive properties and interferes with its interaction to extracellular matrix proteins. Mol Cancer Res **5**, 309–320, doi:10.1158/1541-7786.MCR-06-0353 (2007).
10. Saitou, M. *et al.* MUC4 expression is a novel prognostic factor in patients with invasive ductal carcinoma of the pancreas. J Clin Pathol **58**, 845–852, doi:10.1136/jcp.2004.023572 (2005).
11. Hirono, S. *et al.* Molecular markers associated with lymph node metastasis in pancreatic ductal adenocarcinoma by genome-wide expression profiling. Cancer Sci **101**, 259–266, doi:10.1111/j.1349-7006.2009.01359.x (2010).

12. Moniaux, N., Junker, W. M., Singh, A. P., Jones, A. M. & Batra, S. K. Characterization of human mucin MUC17. Complete coding sequence and organization. J Biol Chem **281**, 23676–23685, doi:10.1074/jbc.M600302200 (2006).
13. Senapati, S. *et al.* Expression of intestinal MUC17 membrane-bound mucin in inflammatory and neoplastic diseases of the colon. J Clin Pathol **63**, 702–707, doi:10.1136/jcp.2010.078717 (2010).
14. Yang, B. *et al.* Mucin 17 inhibits the progression of human gastric cancer by limiting inflammatory responses through a MYH9-p53-RhoA regulatory feedback loop. J Exp Clin Cancer Res **38**, 283, doi:10.1186/s13046-019-1279-8 (2019).
15. Kitamoto, S. *et al.* DNA methylation and histone H3-K9 modifications contribute to MUC17 expression. Glycobiology **21**, 247–256, doi:10.1093/glycob/cwq155 (2011).
16. Kitamoto, S. *et al.* Expression of MUC17 is regulated by HIF1alpha-mediated hypoxic responses and requires a methylation-free hypoxia responsible element in pancreatic cancer. PLoS One **7**, e44108, doi:10.1371/journal.pone.0044108 (2012).
17. Luu, Y. *et al.* Human intestinal MUC17 mucin augments intestinal cell restitution and enhances healing of experimental colitis. Int J Biochem Cell Biol **42**, 996–1006, doi:10.1016/j.biocel.2010.03.001 (2010).
18. Lange, T., Samatov, T. R., Tonevitsky, A. G. & Schumacher, U. Importance of altered glycoprotein-bound N- and O-glycans for epithelial-to-mesenchymal transition and adhesion of cancer cells. Carbohydr Res **389**, 39–45, doi:10.1016/j.carres.2014.01.010 (2014).

Tables

Table 1. Clinicopathological characteristics of pancreatic cancer patients selected for MUC17 staining.

Clinicopathological characteristics of the patients

Variable	PDAC+OJ (n=20)		PDAC (n=21)		NE (n=7)		NORMAL (n=4)	
	n	(%)	n	(%)	n	(%)	n	(%)
Gender	11	(55.0)	12	(57.0)	6	(86.0)	1	(25.0)
• Male • Female	9	(45.0)	9	(43.0)	1	(14.0)	3	(75.0)
Age	7	(35.0)	8	(38.0)	3	(43.0)	4	(100.0)
• 65 • ≥ 65	13	(65.0)	13	(62.0)	4	(57.0)	0	(0.0)
Location of primary tumor								
• Papilla of Vater	2	(10.0)	0	(0.0)	0	(0.0)		
• Head	18	(90.0)	17	(80.0)	3	(43.0)		
• Head/Body	0	(0.0)	0	(0.0)	1	(14.0)		
• Body	0	(0.0)	2	(10.0)	1	(14.0)		
• Tail	0	(0.0)	2	(10.0)	2	(29.0)		
Hystological type								
• Well differentiated	1	(5.0)	4	(19.0)	1	(14.0)		
• Moderately differentiated	13	(65.0)	12	(57.0)	6	(86.0)		
• Poorly differentiated	6	(30.0)	5	(24.0)	0	(0.0)		
Stage of the cancer	3	(15.0)	5	(24.0)				
• II.	9	(45.0)	9	(43.0)	6	(86.0)		
• III.	8	(40.0)	7	(33.0)	1	(14.0)		
• IV.								
Lymphatic invasion		(80.0)	13	(62.0)	7	(100.0)		
• Negative	16	(20.0)	8	(38.0)	0	(0.0)		
• Positive	4							
Metastasis								
• Lung	1	(5.0)	2	(10.0)	0	(0.0)		
• Liver								

• Colon	3	(15.0)	5	(24.0)	2	(29.0)
• Gall bladder	0	(0.0)	0	(0.0)	0	(0.0)
	1	(5.0)	0	(0.0)	0	(0.0)

Table 2. Clinicopathological characteristics of pancreatic cancer patients selected for serum treatment.

Clinicopathological characteristics of the patients

Variable	PDAC+OJ (n=10)		PDAC (n=5)			NORMAL (n=14)		
	n	(%)	n	(%)	p value	n	(%)	p value
Gender	5	(50.0)	2	(40.0)		6	(42.9)	
• Male • Female	5	(50.0)	3	(60.0)	0.7376	8	(57.1)	0.9930
Age	2	(20.0)	0	(0.0)		10	(71.0)	
• 65 • ≥65	8	(80.0)	5	(100.0)	0.5877	4	(29.0)	0.7125
Location of primary tumor	3	(30.0)	0	(0.0)				
• Papilla of Vater	4	(40.0)	5	(100.0)				
• Head • Head/Body	2	(20.0)	0	(0.0)				
• Body	1	(10.0)	0	(0.0)				
• Tail	0	(0.0)	0	(0.0)	0.4369			
Hystological type	0	(0.0)	0	(0.0)	0.5599			
• Well differentiated	7	(70.0)	5	(100.0)				
• Moderately differentiated	3	(30.0)	0	(0.0)				
• Poorly differentiated								
Stage of the cancer	0	(0.0)	0	(0.0)				
• II.	4	(40.0)	4	(80.0)				
• III. • IV.	6	(60.0)	1	(20.0)	0.4456			
Lymphatic invasion		(70.0)	5	(100.0)				
• Negative	7	(30.0)	0	(0.0)	0.5166			
• Positive	3							
Metastasis	0	(0.0)	0	(0.0)				
• Lung	4	(40.0)	3	(60.0)				
• Liver • Colon	1	(10.0)	2	(30.0)				
• Gall bladder	0	(0.0)	0	(0.0)	0.6540			

Figures

Figure 1

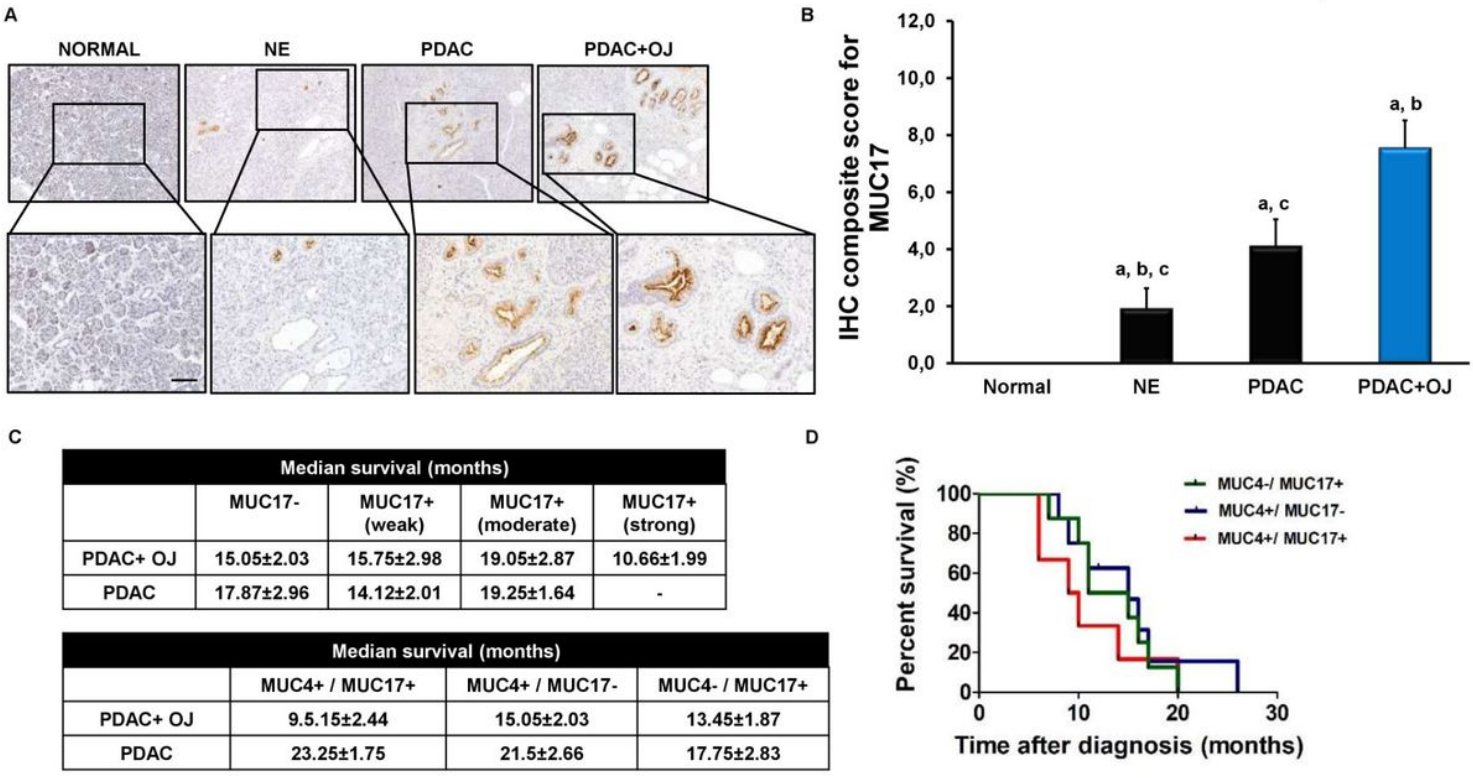

Median survival (months)				
	MUC17-	MUC17+ (weak)	MUC17+ (moderate)	MUC17+ (strong)
PDAC+ OJ	15.05±2.03	15.75±2.98	19.05±2.87	10.66±1.99
PDAC	17.87±2.96	14.12±2.01	19.25±1.64	-

Median survival (months)			
	MUC4+ / MUC17+	MUC4+ / MUC17-	MUC4- / MUC17+
PDAC+ OJ	9.5.15±2.44	15.05±2.03	13.45±1.87
PDAC	23.25±1.75	21.5±2.66	17.75±2.83

Figure 1

Expression of MUC4 and -17 in human pancreatic samples and survival curves of PDAC patients. (**A**) Representative immunohistochemical stainings show the presence of MUC17 in human pancreatic samples. (**B**) Composite scores of human pancreatic samples stained with anti-MUC17 antibody. Data represent the mean ± SEM of 23–25 specimens/4–21 patients each group. a = $p \leq 0.05$ vs. normal, b = $p \leq 0.05$ vs. PDAC, c = $p \leq 0.05$ vs. PDAC+OJ. Scale bar represents 100 µm. (**C**) Median survival and (**D**) survival curves of PDAC patients. MUC4+/MUC17+ vs MUC4-/MUC17+ Log rank: 0.4268, MUC4+/MUC17+ vs MUC4+/MUC17- Log Rank: 0.04378, MUC4-/MUC17+ vs MUC4+/MUC17- Log Rank: 0.5672. PDAC: pancreatic ductal adenocarcinoma; OJ: obstructive jaundice; NE: neuroendocrine tumor.

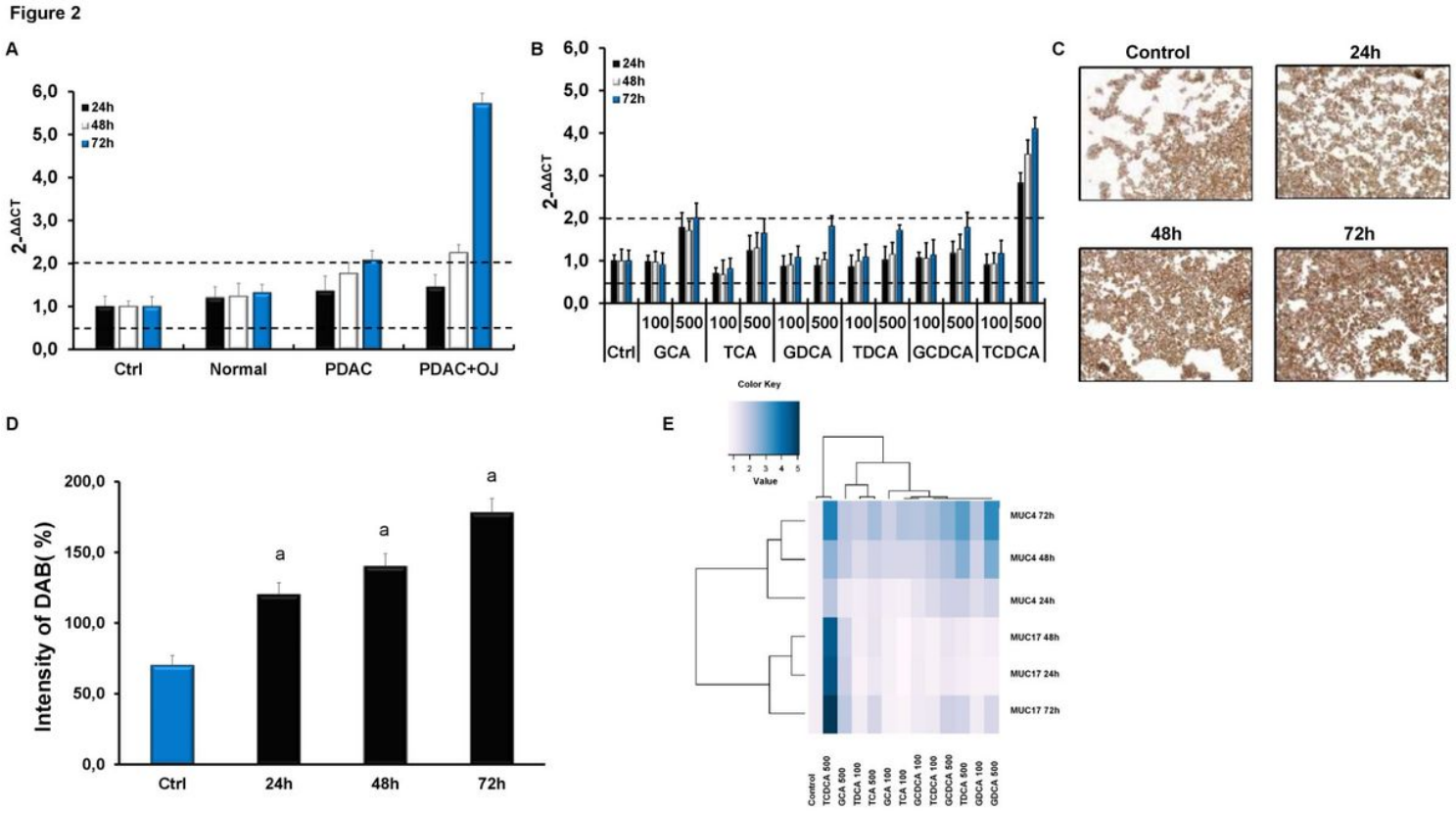

Figure 2

Effects of bile acid treatment on the mRNA and protein expression of mucins in pancreatic ductal cells. Capan-1 cells treated with human serum obtained from healthy volunteers and pancreatic ductal adenocarcinoma patients (**A**) and with different bile acids (BAs) (**B**) for 24, 48, and 72 hours, and the relative gene expressions of MUC17 were investigated by real-time polymerase chain reaction. (**C**) Representative immunofluorescence staining of Capan-1 cells shows the expression of MUC17 after the treatment with taurochenodeoxycholic acid (TCDCA; 500 μM) for 24, 48 and 72 hours. (**D**) Quantification of MUC17 protein expression. Specimens were scanned by a Olympus IX83-based system, and DAB staining intensities were analyzed by ImageJ software. Data represent the mean ± SEM of three independent experiments. a = $p \leq 0.05$ vs. Control. (**E**) The cluster analysis and dendrogram show the difference between the effect of BAs treatment at different concentrations and time points on MUC4 and MUC17 expression. Blue and white colors indicate high and low expression, respectively. (Values represent the fold change in the gene expression level of MUC genes). Data represent the mean ± SEM of three independent experiments. GCA: glycocholic acid, TCA: taurocholic acid, GDCA: glycodeoxycholic acid, TDCA: taurodeoxycholic acid, GCDCA: glycochenodeoxycholic acid, TCDCA: taurochenodeoxycholic acid.

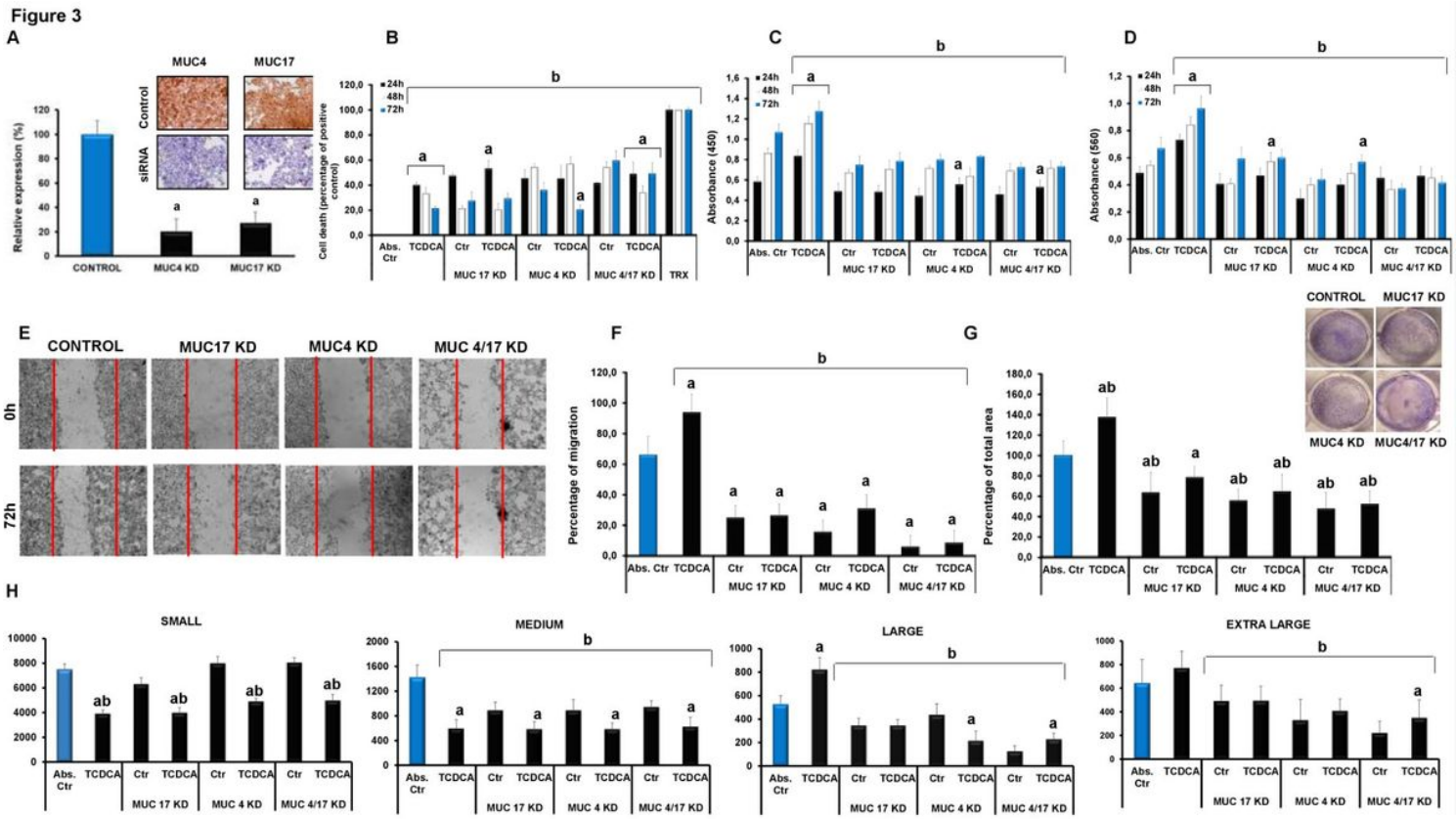

Figure 3

Knockdown of MUC4 and -17 in Capan-1 cells. (A) The expression levels of MUC4 and -17 was investigated by reverse transcription-polymerase chain reaction and immunohistochemistry in the control cells and cells treated with specific siRNAs. The rates of viability (**B**), proliferation (**C**), and adhesion (**D**) were determined at 24, 48, and 72 hours, whereas migration (**E** and **F**) and colony formation (**G** and **H**) at 72 hours. Data represent the mean ± SEM of three independent experiments. a=$p \leq 0.05$ vs. Control, b=$p \leq 0.05$ vs. abs. Control. TCDCA: taurochenodeoxycholic acid, TRX: Triton-X-100.